INFLUENCE OF DIFFERENT DISTRIBUTION PATTERNS OF HOLES ON SINGLE MICRO-PERFORATED PANEL SOUND ABSORPTION BEHAVIOUR

Hoda Mohamed Abo Dorra[*1], Mohamed Abd-Elbasseer[†2], Abd Elfattah A Mahmoud[‡2] , and Hatem Kh. Mohamed[♦2]
[1]*Physics Department, Faculty of Women for Arts, Science and Education, Ain Shams University, Cairo, Egypt*
[2]*Acoustics Laboratory, National Institute of Standards (NIS), Giza, Egypt.*

Résumé

Les panneaux micro-perforés sont devenus ces derniers temps une option valable d'absorption acoustique à large bande. Leur champ d'application est large puisqu'ils sont prometteurs pour l'absorption de l'énergie sonore dans plusieurs applications, telles que l'automobile, les systèmes de chauffage, de ventilation et de climatisation, les murs antibruit, etc. Cette étude étudie l'effet de différents modèles de distribution des trous, du taux de perforation, de la profondeur de l'entrefer et de la géométrie des trous sur le comportement d'absorption acoustique des panneaux micro-perforés individuels. Quatre modèles de distribution différents (cercle, carré, triangle et aléatoire) des orifices sont conçus et fabriqués sur une surface de tôle d'une épaisseur de 1 mm avec un diamètre de trou de 1 mm et une profondeur d'entrefer de 100 mm entre le panneau et la paroi arrière. Chaque motif de distribution des quatre différents motifs a été perforé avec sept rapports de perforation (0,12 %, 0,36 %, 0,48 %, 0,60 %, 0,84 %, 1,1 % et 1,9 %) Les mesures ont été effectuées à l'aide du tube d'impédance à deux microphones dans la gamme des basses fréquences de 100 Hz à 1000 Hz. Bien que les résultats n'aient pas révélé de différence significative entre les coefficients d'absorption des différents modèles de trous pour tous les rapports de perforation, le modèle aléatoire est légèrement plus élevé que les autres modèles de distribution. L'augmentation de la profondeur de l'entrefer a amélioré le coefficient d'absorption acoustique moyen dans la gamme de fréquences allant de 160 Hz à 630 Hz de 0,29 à 0,51. De plus, le changement de la géométrie des trous, qui est passée du cercle au carré et au triangle, a amélioré le coefficient d'absorption acoustique d'environ 11 % et 12 %. On obtient une bonne cohérence entre les calculs théoriques et les résultats expérimentaux.

Mots-clés : Absorbeur à panneau microperforé, modèle de distribution, géométrie des trous, modèle Maa.

Abstract

Micro-perforated panels have become a valid broadband sound absorber option lately. Their applicability is wide since they are promising for absorbing sound energy for several applications, such as automotive, HVAC systems, noise barriers, etc. This study investigates the effect of different distribution patterns of holes, perforation ratio, air gap depth, and the hole geometry on single micro-perforated panels' sound absorption behavior. Four different distribution patterns (Circle, Square, Triangle, and Random) of orifices are designed and fabricated on a surface of sheet metal of thickness 1 mm with hole diameter 1mm, and air gap depth between the panel and the back wall 100 mm. Each of the four different distribution patterns was perforated with seven perforation ratios (0.12%, 0.36%, 0.48%, 0.60%, 0.84%, 1.1%, and 1.9%).The measurements were carried out using the two-microphone impedance tube in the low-frequency range from 100 Hz to 1000 Hz. Although the results revealed no significant difference between the absorption coefficients of different holes' patterns at all the perforation ratios, the random pattern is slightly higher than other distribution patterns. Increasing the air gap depth improved the average sound absorption coefficient in the frequency range from 160 Hz to 630 Hz from 0.29 to 0.51. Moreover, changing the hole geometry from circle to square and triangle enhanced the sound absorption coefficient by about 11 % and 12 %. Good consistency between the theoretical calculations and the experimental results is obtained.

Keywords: Micro-Perforated Panel Absorber, Distribution Pattern, Hole Geometry, Maa Model.

1 Introduction

In the form of a micro-perforated panel (MPP), the sound absorber has drawn researchers ' concern because of its benefits over porous absorbent materials. It has been recognized as the next generation of conventional absorbing material because it has the merits of an excellent sound absorption performance, high strength, excellent wash ability, eco-friendly, and can be used in a harsh environment [1, 2]. Moreover, they can be designed to provide wideband sound absorption for a specific frequency range by changing MPP parameters such as the hole diameter (d), panel thickness (t), perforation ratio (σ), and the cavity depth (D).

The essential acoustic concept of MPP is strain forward, it is to produce a surface with a built-in damping which concretely absorbs sound waves. To realize this, the acoustic impedance of a MPP absorber is normally tuned to be of the order of the in air). When the oscillating air molecules penetrate the MPP, the friction between the air in motion and the

[*] hatemacoustics@gmail.com
[†] mbacir@yahoo.com
[‡] yy_abd_elfattah@yahoo.com
[♦] hatem_teleb@yahoo.com

surface of the MPP dissipates the acoustical energy Maa [1, 3, 4] first proposed the MPP concept, its theoretical basis, and design guidelines. MPP is a thin panel or membrane made of wood, plastic, or metal with thickness $t \leq 1.0$ mm, perforation ratio $\sigma \leq 1.0$ %, and air gap of rigid back [5]. Hua and Herrin set the perforation ratio to 5.0 % [6]. Now MPP is widely used in different applications such as automotive, room acoustics, HVAC systems, compressors, turbines, and window systems [7-11]. When compared to the traditional porous and fibrous sound absorber materials, high sound absorption coefficients can be achieved with a relatively small thickness. MPP absorbers' sound absorption mechanism is due to the oscillatory air movement through MPP's small orifices, resulting in dissipated sound energy. It has been proposed that many small perforations should be used instead of a few large apertures to achieve more excellent absorption [6]. Maa Dah-You [11] studied the sound absorption coefficient of micro-perforated panels with a sub-millimeter size of diameter (0.5–1) mm, to provide enough acoustic resistance and low acoustic mass reactance, which are necessary for wideband sound absorber, without using additional fibrous or porous materials. To enhance the acoustic performance of the single MPP absorbers, numerous experiments and trials have been suggested. K. Sakagami [12] revealed that the honeycomb in the air cavity of an MPP absorber has not only made the MPP stiffer, but it has also improved the sound absorption performance, especially at low frequencies. Liu and Herrin [13] investigated that partitioning the air gap by using the honeycomb only, increases the overall sound attenuation by about 4 dB. Sakagami [14] showed that the absorption peak value becomes slightly lower by inserting a porous absorbent layer into the back cavity. Liu [13] concluded that MPP's attachment with porous material in front of the air gap broadened the sound absorption frequency range because the porous material layer damped the air resonance in the air gap. Iman Falsafiet [15] concluded that the absorption's magnitude and bandwidth are rely on the hole diameter and the perforation ratio rather than the panel thickness. Moreover, the cavity depth is the parameter that controls the position of the resonance frequency of MPP. A literature gap was found on the influence of different perforation patterns and perforation geometry on MPP's sound absorption [16-18]. They studied only the heterogeneity (unevenly) distribution of orifices over the panel surface. In contrast, this study aims to investigate the influence of four different distribution patterns of perforations (Circle, Square, Triangle, and Random), perforation ratio, air gap depth, and the hole geometry on the acoustic performance of single MPPs to attain the best distribution pattern, which provides the optimum absorption as a good solution for the low-frequency noise problems.

The paper is organized as follows: Section 2 presents the theoretical background of single MPP.
.Section 3 focuses on the experimental arrangement of the used method and the MPP samples preparation. Section 4 describes the results obtained and the explanation for both the experimental results and the theoretical calculations.

2 Theoretical background of single MPP

Micro-perforated panel sound-absorbing construction consists of a thin panel perforated with a large number of sub-millimeter holes together with an air space behind it. The structure and its equivalent circuit are shown in figure 1.

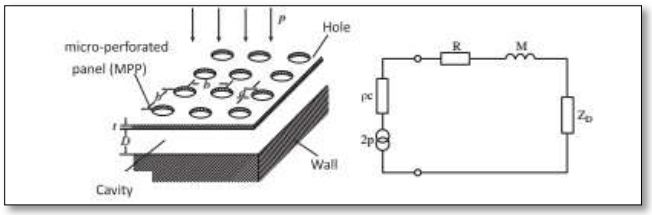

Figure 1: Micro-Perforated panel sound absorber construction and its equivalent circuit.

The holes of MPP may be considered a lattice of short narrow tubes separated by distances much larger than their diameters but small compared to the impinging sound's wavelength. For the sound wave's normal sound incidence on the micro-perforated panel, the wave motion in all the short tubes is in phase and additive. Maa [1] derived the relative (to the characteristic impedance ρc in the air) acoustic impedance of MPP with end corrections:

$$Z_{MPP} = (R + jM)/\rho C = r + j\omega m. \quad (2.1)$$

Where r and m are the normalized specific acoustic resistance (the real part) and the normalized acoustic reactance (the imaginary part), respectively, and ω (equal to 2πf) is the angular frequency.

$$r = \frac{32\eta t}{\sigma \rho_0 C_0 d^2}\left(\sqrt{1+\frac{x^2}{32}} + \frac{\sqrt{2}}{8}\frac{xd}{t}\right); \quad (2.2)$$

$$m = \frac{t}{\sigma C_0}\left(1+\left(9+\frac{x^2}{2}\right)^{-0.5}\right)+0.85\frac{d}{t}; \quad (2.3)$$

$$X = d\sqrt{\omega\rho_0/4\eta}\,. \quad (2.4)$$

Here, η is the air's viscosity coefficient, $1.506*10^{-5}$ m^2/s, ρ is the air density, 1.225 Kg/m^3, x is the perforation panel constant d, t is the hole diameter and the panel thickness, respectively. In this study, the holes are not evenly distributed on the total panel area (holes localized in a part of the panel area), assuming cylindrical perforations with the same diameter d, the perforation ratio is given by [19]

$$\sigma = \frac{n*\pi*d^2}{4S_p}. \quad (2.5)$$

Where n is the number of holes on the panel, S_p is the panel area. The normalized specific acoustic impedance of air cavity with thickness D behind the MPP panel is determined by [20]

$$Z_D = -jcot\left(\frac{\omega D}{C}\right). \quad (2.6)$$

And the total specific acoustic impedance Z_{total} of a conventional single MPP under normal incidence can be determined by [20]

$$Z_{total} = Z_{MPP} + Z_D \quad (2.7)$$

By having the total impedance of MPP, the sound absorption coefficient can be calculated from [15]

$$A = \frac{4r}{(1+r^2)+(\omega m - \cot(\omega D/C))^2} \quad (2.8)$$

And the maximum absorption coefficient is calculated by

$$\alpha_{max} = \frac{4r}{(1+r)^2} \quad (2.9)$$

3 Experimental arrangement

3.1 Experimental setup

Following ASTM 1050-12 standard [21], the acoustic absorption was experimentally measured using a two-microphone impedance tube technique. The measurements were carried out at 22.0^0 C laboratory ambient temperature and 56 % relative humidity. Figure 2 displays the laboratory test setup, where the B&K impedance tube type 4206 was used to measure the samples' sound absorption coefficient. The impedance tube's internal diameter was 100 mm, and the acoustic properties were measured in the frequency range from 100 to 1000 Hz. In this method, a loudspeaker that produced a random sound signal was put at one end, and the sample was mounted on the sample holder at the other end. The samples were fitted firmly with the inner diameter of the tube. The edges between the panel and the walls of the tube were sealed by clay to prevent leakage. Finally, the normal incidence sound absorption coefficient is measured using a software program.

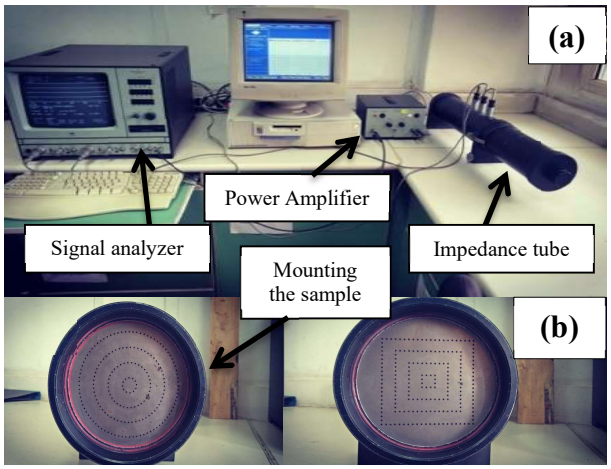

Figure 2: (*a*) B&K 4206 Impedance tube measurement setup, (*b*) Mounting of the sample inside the tube.

3.2 MPP samples preparation

In this study, 34 samples have been used; the samples are divided into 28 samples related to the different distribution patterns of holes and six samples related to the different hole geometry. Samples are in the form of a 1mm metal sheet of diameter 100mm.The samples are named (A, B, C, D, E, F, and G) with perforation ratios are 0.12%, 0.36%, 0.48%, 0.6%, 0.84%, 1.1% and 1.9% respectively [22, 23]. The holes in each sample were distributed with four different patterns (Circle, Square, Triangle, and Random), as shown in figure 3. Maa [1] clearly states that the open area ratio's value is important, noting that while a small change of its value is usually permitted, the exact value is required for a perfect model prediction [24]. So, the parameters of thickness, hole diameter, and the cavity depth are kept constant for groups A to G. AutoCAD software was used to draw the different distribution patterns of orifices on the surface of the panel. The orifices have been perforated using laser drilling with diameter 1mm and with the 7 previously listed perforation ratios. Figure 3 shows the four different distribution patterns at different perforation ratios.

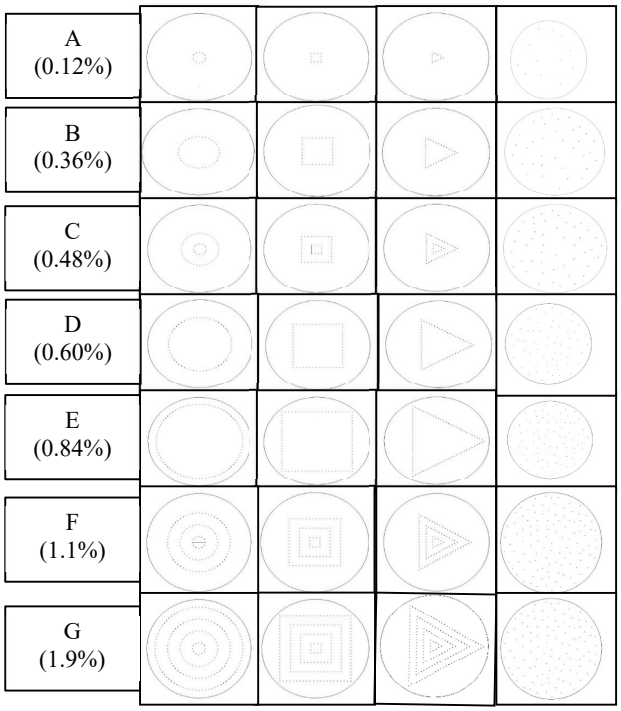

Figure 3: Schematic diagram of different distribution patterns of orifices at each perforation ratio.

4 Parametric survey

The perforation ratio's influence on single MPPs' sound absorption coefficient figure 4 for the same panel thickness, hole diameter, and cavity depth, as listed in Table 1.

Table 1: Geometrical properties of MPPs.

Spec.	Sample	t (mm)	d (mm)	D (mm)	σ (%)
Changing Perforation Ratio	A	1	1	100	0.12
	B				0.36
	C				0.48
	D				0.60
	E				0.84
	F				1.1
	G				1.9

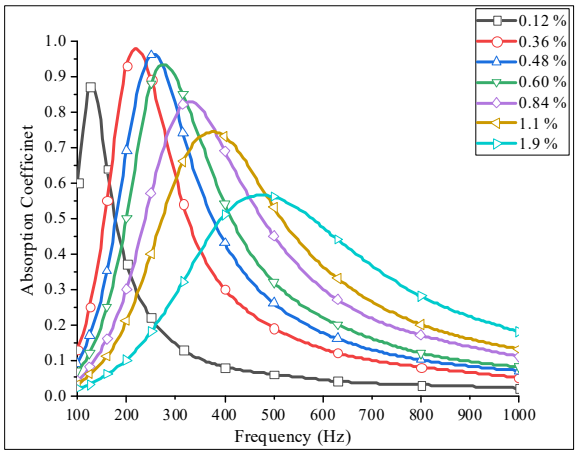

Figure 4: Sound absorption at different perforation ratios – Maa's Model.

Table 2: Absorption coefficient and acoustic resistance characteristics of single MPPs for Different perforation ratios.

σ (%)	f_0 (Hz)	α_{max}	r
0.12	125	0.87	2.1
0.36	200	0.93	0.8
0.48	250	0.96	0.7
0.60	250	0.90	0.5
0.84	315	0.82	0.4
1.1	400	0.73	0.3
1.9	500	0.56	0.2

Considering the perforation ratio in Equation (2.5), this parameter affects the acoustic impedance resistance. The maximum absorption needs the resistance part to be close to 1, as clarified by Equation (2.9). Table 2 shows that the MPP with resistance part close to 1 has a higher absorption coefficient. It is revealed from a parametric survey that the acoustic resistance value close to 1±0.5 allows the absorption coefficient value of the MPP panel (α = 0.90 - 0.96) [25]. In contrast, the acoustic resistance value higher or smaller than that value will result in a lower absorption coefficient.

5 Result and discussion

5.1 Effect of perforation ratio

Figure 5 reveal the comparison between the measured sound absorption coefficients of 28 samples. The air gap between the back wall and the samples was kept constant at 100 mm.

From figures (5-1) to (5-7), it is found that, at all perforation ratios, there is no significant difference between the measured sound absorption coefficients of the four different distribution patterns of orifices. In other words, at each perforation ratio, the absorption coefficients of four distribution patterns have the same behavior and approximately the same amplitudes. It is also revealed that, when the perforation ratio increased, the resonance frequency shifted to higher frequencies. However, increasing the perforation ratio broadened the frequency of the sound absorption; the amplitude of the absorption coefficient decreased. This was due to the decrease in the panel's acoustic mass, which consequently reduces the acoustic resistance. By comparing all distributions patterns of holes at all perforation ratios, it is revealed that the Random pattern is slightly higher than other distribution patterns, and this may be due to:

1. The random distribution of holes on the sample surface covers most of the sample surface, and thus the absorption area over the sample surface increases.

2. By comparing the random distribution with other distribution patterns such as the circular, triangle, and square distribution, for instance, in the case of 0.6 %, it can be seen that the holes are concentrated in a specific area on the sample surface. The rest of the sample surface is a reflective part; accordingly, a great part of the incident sound energy on the sample is reflected. In contrast to the random distribution in which the holes are distributed larger on the sample's surface, consequently, the bulk of the incident sound energy is absorbed.

Table 3: Theoretical and experimental resonance frequency and maximum absorption coefficient at different patterns and different perforation ratios.

σ (%)	Theo.		Exp.							
			Circle		Square		Triangle		Random	
	f_0	α_{max}	f_0	α_{max}	f_0	α_{max}	f_0	α_{max}	f_0	α_{max}
0.12	125	0.87	125	0.9	125	0.91	125	0.88	125	0.92
0.36	200	0.93	200	0.96	200	0.96	200	0.95	200	0.97
0.48	250	0.96	250	0.98	250	0.98	250	0.97	250	0.94
0.60	250	0.90	250	0.94	250	0.94	250	0.87	250	0.98
0.84	315	0.82	315	0.89	315	0.89	315	0.87	315	0.94
1.1	400	0.73	400	0.79	400	0.79	400	0.8	400	0.82
1.9	500	0.56	500	0.66	500	0.62	500	0.61	500	0.69

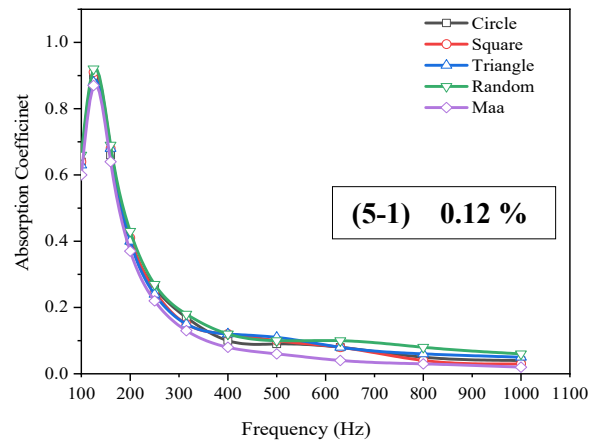

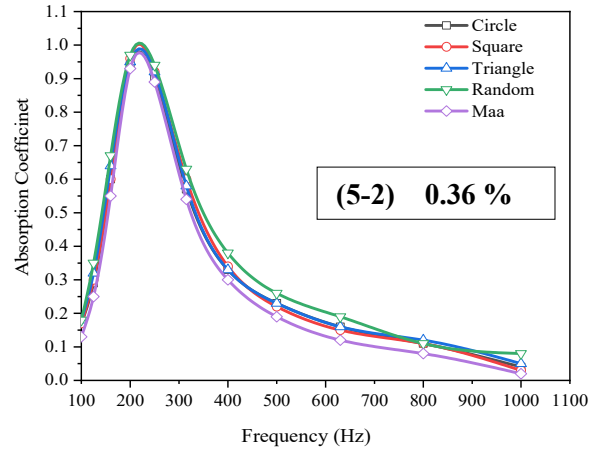

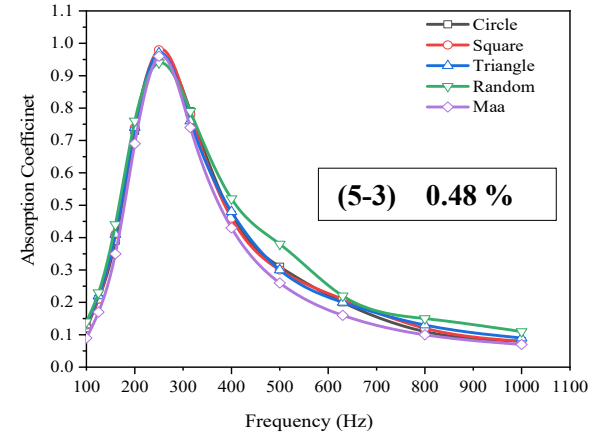

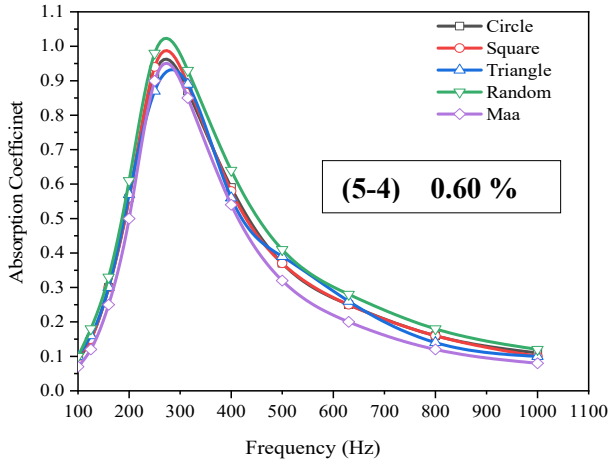

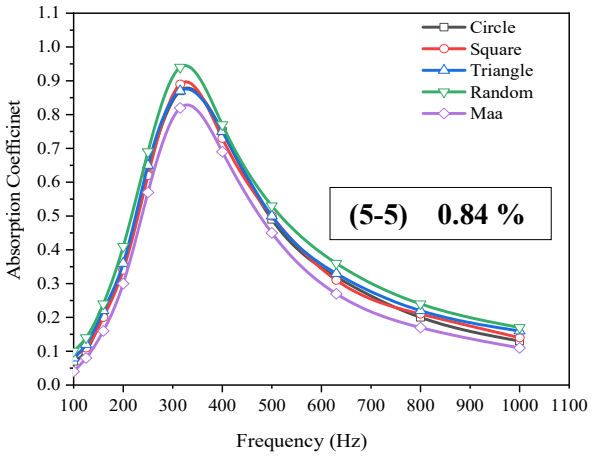

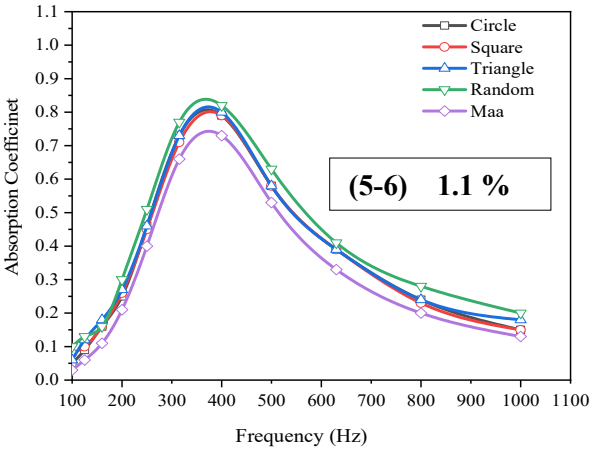

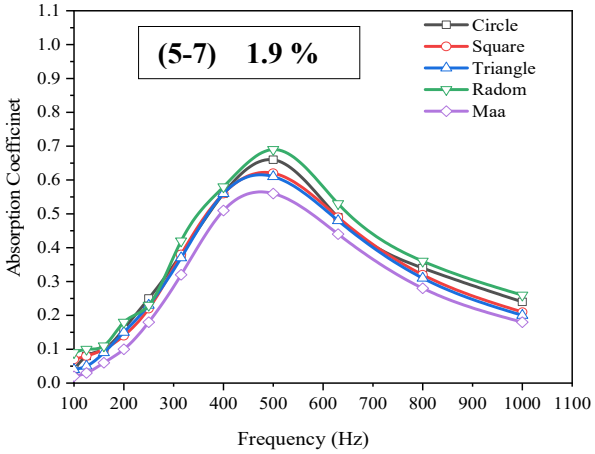

Figure 5: Measured sound absorption coefficient of different samples at different patterns of holes.

It is also demonstrated that there is a proper consistency between the theoretical calculations using Maa's model and the experimental results. Also, there is a coincidence between the calculated resonance frequencies, and those found experimentally at different distribution patterns circle, square, triangle, and random patterns. Moreover, it is revealed that the experimental results have wider frequency bandwidths and higher absorption amplitudes than the theoretical calculations. The inconsistencies between the experimental results and the theoretical calculations could be ascribed to the accompanying reasons: (i) the laser-drilled orifices were not

perfectly circular in shape, as shown in figure 6 [26]. (ii) The shavings inside the perforations due to the drilling process are not easily observable for tiny perforations, and consequently, this may alter or change the MPP acoustic behavior [24]. Since all the drilled holes were not consistent and not equal to the designed values of 1mm. (iii) the theory did not consider the variation in the kinematic viscosity coefficient of air μ and the sound speed in air C_0 due to the temperature change in experiments. (iv) The depth of the air gap in the measurements was challenging to be completely consistent with the theoretical values [2].

Figure 6: Profile projector image of laser drilled perforations in imperfect circular shapes.

Figure 7 below compares between the random distribution pattern at each perforation ratio.

However, increasing the perforation ratio broadened the sound absorption, the value of the sound absorption coefficient decreased. The average absorption coefficient of Random pattern at perforation Ratios A, B, C, D, E, F, and G in the frequency range from 100 to 630 Hz are 0.39, 0.51, 0.49, 0.50, 0.46, 0.43, and 0.33, respectively. This means that the samples which provide average sound absorption coefficients above 0.5 are B and D. Furthermore, the maximum absorption coefficient which occurs at the resonance frequency increased by increasing the perforation ratio to a particular value of 0.60 % then it decreases after this ratio, and this coincides with Maa's theory which stated that the optimum sound absorption occurs at perforation ratio ≤ 1.0 %.

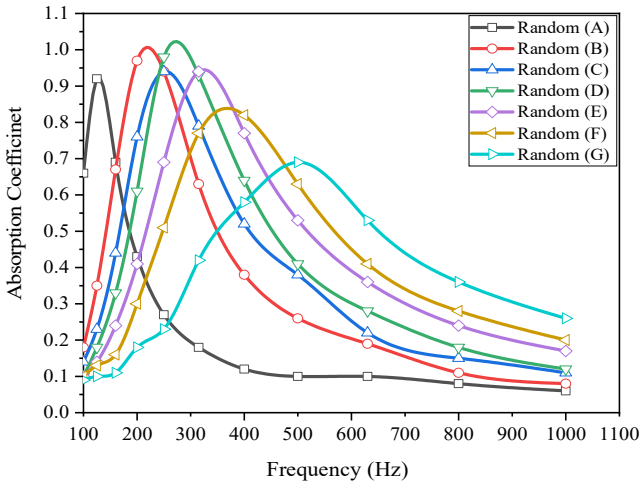

Figure 7: Measured sound absorption coefficient of different samples at Random Pattern.

5.2 Effect of air gap depth

The sound absorption coefficient was experimentally measured at air gap depths of 20 mm, 50 mm, and 100 mm for B and D samples, which have the highest average sound absorption coefficient at random patterns, and the findings are shown in figures 8 and 9.

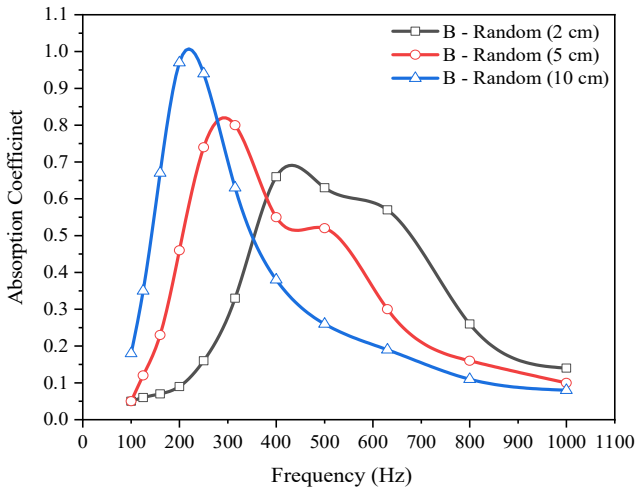

Figure 8: Sound absorption coefficient of sample B at different cavity depths.

It is revealed from figures 8 and 9 that increasing the air gap depth results in shifting the resonance frequency to lower frequencies. The explanation behind that is the MPP and the air gap act as a mass-spring system where the MPP represents the mass, and the cavity represents the spring. Increasing the air cavity depth reduces the stiffness of the spring [26], which in turn shifted the resonance frequency from 400 Hz to 200 Hz in case of sample B and from 630 to 250 Hz in case of sample D. Furthermore, increasing the air gap depth improved the average sound absorption coefficient in the frequency range from 160 Hz to 630 Hz from 0.29 to 0.51 in case of sample B and from 0.30 to 0.50 in case of sample D.

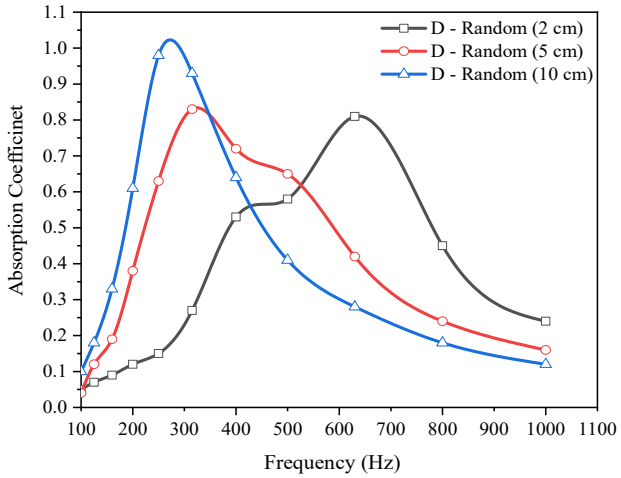

Figure 9: Sound absorption coefficient of sample D at different cavity depths

5.3 Effect of hole geometry

The influence of hole geometries on single MPPs' sound absorption performance at different distribution patterns of holes at a perforation ratio of 0.6 % are presented in figures 10,11 and 12.

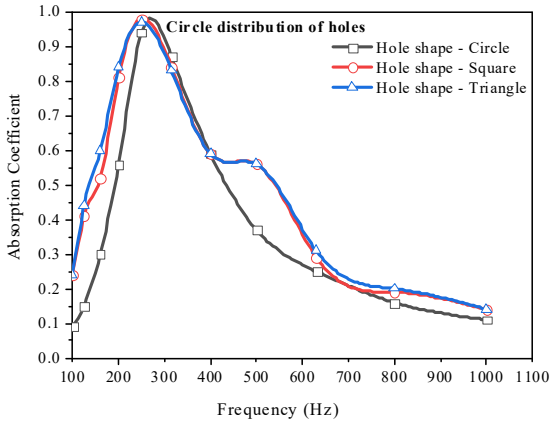

Figure 10: Measured sound absorption coefficient of different hole geometries at Circle distribution pattern.

It is demonstrated from figures 10,11 and 12 that the sound absorption coefficient at square and triangle hole geometries is higher than that of circle hole geometry at different distribution patterns of holes. In other words, in the case of circle distribution of holes, the average sound absorption coefficient is 0.55, 0.66, and 0.67 for circle, square, and triangle hole geometry respectively in the frequency range from 160 to 630 Hz. which means that, when the hole geometry changed from circle to square and triangle, the sound absorption coefficient enhanced by about 11 % and 12 % respectively.

In triangle hole distribution, the average sound absorption coefficient is 0.55, 0.65, and 0.65 for circle, square, and triangle hole shape, respectively, in the frequency range from 160 to 630 Hz, which means that there was an increment of about 10% when the hole shape changes from circle to square and triangle.

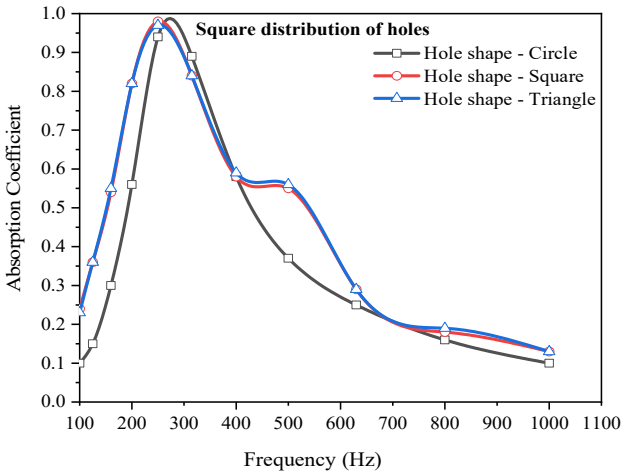

Figure 11: Measured sound absorption coefficient of different hole geometries at Square distribution pattern.

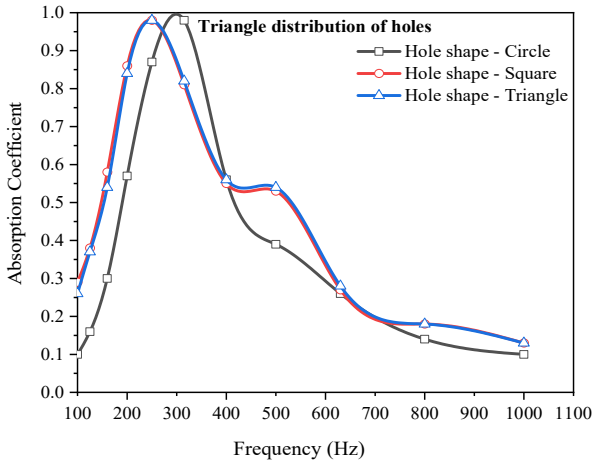

Figure 12: Measured sound absorption coefficient of different hole geometries at Triangle distribution pattern.

6 Conclusion

The influence of different distribution patterns of orifices, air gap depth, perforation ratio, and the hole geometry on single MPPs' sound absorption behavior is investigated. It is concluded that there is no significant difference between the sound absorption coefficients of the different patterns of holes at all perforation ratios. In other words, at all perforation ratios, the absorption coefficients of the four distribution patterns, circle, square, triangle, and Random, have the same behavior and approximately the same amplitudes. Perforation ratios of 0.36 and 0.60 % at a Random pattern provided the highest absorption coefficients where the average sound absorption coefficient was 0.51 and 0.50, respectively, in the frequency range from 160 Hz to 630 Hz. This study also revealed that increasing the air gap depth improved the average sound absorption coefficient in the frequency range from 160 Hz to 630 Hz from 0.29 to 0.51 at perforation ratio 0.36 % and from 0.30 to 0.50 at perforation ratio 0.60 %. Changing the hole geometry from circle to square and triangle enhanced the sound absorption coefficient of about 11 % and 12 %,

respectively. Furthermore, a good consistency between the experimental results and the theoretical calculations using Maa's model is obtained.

References

[1] Maa, D.-Y., Potential of microperforated panel absorber. the Journal of the Acoustical Society of America, 1998. 104(5): p. 2861-2866.

[2] Yang, X., et al., Optimal design and experimental validation of sound absorbing multilayer microperforated panel with constraint conditions. Applied Acoustics, 2019. 146: p. 334-344.

[3] Maa, D.-Y., Theory and design of microperforated panel sound-absorbing constructions. Scientia Sinica, 1975. 18(1): p. 55-71.

[4] Maa, D.-Y., Microperforated-panel wideband absorbers. Noise control engineering journal, 1987. 29(3): p. 77-84.

[5] Sakagami, K., et al., Double-leaf microperforated panel space absorbers: A revised theory and detailed analysis. Applied Acoustics, 2009. 70(5): p. 703-709.

[6] Hua, X., D. Herrin, and P. Jackson, Enhancing the performance of microperforated panel absorbers by designing custom backings. SAE International Journal of Passenger Cars-Mechanical Systems, 2013. 6(2013-01-1937): p. 1269-1275

[7] Matsuno, H., K.M. Kadowaki, and H. Tsuji, Generation II knee bracing for severe medial compartment osteoarthritis of the knee. Archives of physical medicine and rehabilitation, 1997. 78(7): p. 745-749.

[8] Zha, X., H. Fuchs, and H. Drotleff, Improving the acoustic working conditions for musicians in small spaces. Applied acoustics, 2002. 63(2): p. 203-221.

[9] Wu, M.Q., Micro-perforated panels for duct silencing. Noise Control Engineering Journal, 1997. 45(2): p. 69-77.

[10] Kang, J. and M. Brocklesby, Feasibility of applying micro-perforated absorbers in acoustic window systems. Applied Acoustics, 2005. 66(6): p. 669-689.

[11] Maa, D., Practical absorption limits of MPP absorbers. ACTA ACUSTICA-PEKING-, 2006. 31(6): p. 481.

[12] Sakagami, K., et al., Sound absorption characteristics of a honeycomb-backed microperforated panel absorber: Revised theory and experimental validation. Noise Control Engineering Journal, 2010. 58(2): p. 157-162.

[13] Liu, J. and D. Herrin, Enhancing micro-perforated panel attenuation by partitioning the adjoining cavity. Applied Acoustics, 2010. 71(2): p. 120-127.

[14] Sakagami, K., et al., Sound absorption characteristics of a single microperforated panel absorber backed by a porous absorbent layer. Acoustics Australia, 2011. 39(3).

[15] Falsafi, I. and A. Ohadi, Design guide of single layer micro perforated panel absorber with uniform air gap. Applied Acoustics, 2017. 126: p. 48-57

[16] Villamil, H.R., Acoustic properties of microperforated panels and their optimization by simulated annealing. 2012, Universidad Politécnica de Madrid.

[17] Rostand, T., Effects of unevenly distributed holes on the perforated plate sound absorption coefficient. Noise Control Engineering Journal, 2013. 61(6): p. 547-552.

[18] Tayong, R., On the holes interaction and heterogeneity distribution effects on the acoustic properties of air-cavity backed perforated plates. Applied acoustics, 2013. 74(12): p. 1492-1498.

[19] Tayong, R. and P. Leclaire, Experimental investigation of perforations interactions effects under high sound pressure levels. arXiv preprint arXiv:0907.4106, 2009.

[20] Liu, Z., et al., Acoustic properties of multilayer sound absorbers with a 3D printed micro-perforated panel. Applied Acoustics, 2017. 121: p. 25-32.

[21] E-12, A. Standard test method for impedance and absorption of acoustical materials using a tube, two microphones and a digital frequency analysis system. in American Society for Testing and Materials. 2012.

[22] Deacon, M., et al., Analysis of high porosity micro perforated panel using different methods.

[23] Allam, S., Y. Guo, and M. Åbom, Acoustical study of micro-perforated plates for vehicle applications. 2009, SAE Technical Paper.

[24] Tayong, R., On some problems Related to the Fabrication of a Metallic Micro-Perforated Panel for Noise Control Applications.

[25] Prasetiyo, I., J. Sarwono, and I. Sihar, Study on inhomogeneous perforation thick micro-perforated panel sound absorbers. Journal of Mechanical Engineering and Sciences (JMES), 2016. 10(3): p. 2350-2362.

[26] Yang, W., et al., 3D printing of polymeric multi-layer micro-perforated panels for tunable wideband sound absorption. Polymers, 2020. 12(2): p. 360.